Title: Transit Timing and Duration Variations for the Discovery and Characterization of Exoplanets

Eric Agol and Daniel C. Fabrycky

Abstract Transiting exoplanets in multi-planet systems have non-Keplerian orbits which can cause the times and durations of transits to vary. We review the theory and observations of transit timing variations (TTV) and transit duration variations (TDV).

Introduction

Here we discuss some aspects of planetary orbital physics, to set the stage for TTV and TDV. Consider the vector stretching from the star of mass $M_\star$ to the planet of mass M_p to be $\mathbf{r} = (x, y, z)$, with a distance r and direction $\hat{\mathbf{r}}$. The Keplerian potential, $\phi = -GM/r$ (where $M \equiv M_\star + M_p$ and the planet is replaced with a body of reduced mass $\mu \equiv M_\star M_p/(M_\star + M_p)$), is one of only two radial, power-law potentials that gives rise to closed orbits [1]. This means that, in the absense of perturbations, there is a strict periodicity $\mathbf{r}(t+P) = \mathbf{r}(t)$. Moreover, Kepler showed that Tycho Brahe's excellent data for planetary positions were consistent with Copernicus' idea of a heliocentric system only if the planets (including the Earth) followed elliptical paths of semi-major axis a, and one focus on the Sun. Newton was successful at finding the principle underlying such orbits, a force law $\mathbf{F} = \mu\ddot{\mathbf{r}} = -G\mu M r^{-2}\hat{\mathbf{r}}$, which results in a period $P = 2\pi a^{3/2} G^{-1/2}(M_\star + M_p)^{-1/2}$ (i.e. with the a-scaling Kepler found the planets actually obeyed).

Eric Agol
Department of Astronomy, Box 351580, University of Washington, Seattle, WA 98195-1580, USA
e-mail: agol@uw.edu

Daniel C. Fabrycky
Dept. of Astronomy & Astrophysics, University of Chicago, Chicago, IL 60637, USA e-mail: fabrycky@uchicago.edu

[1] the other one, the harmonic potential $-kr$ would only have relevance for collisionless orbits within a homogeneous massive body

This research program was thrown into some doubt by the "Great Inequality," the fact that the orbits of Jupiter and Saturn did not fit the fixed Keplerian ellipse model. This was overcome by the perturbation theory of Lagrange, which resulted in the first characterization of the masses of those planets (check). We can recreate the main effect of this insight by writing an additional force to that of gravity of the Sun:

$$\mathbf{F_1} = -G\mu_1 M r_1^{-2}\hat{\mathbf{r}}_\mathbf{1} + \mathbf{F_{21}}, \tag{1}$$

where we now specify forces and distances explicitly to planet 1, and add a force of planet 2 on planet 1. This latter force consists of two terms:

$$\mathbf{F_{21}} = \mu_1 \ddot{\mathbf{r}}_\mathbf{1} = -G\mu_1 M_2 |r_1 - r_2|^{-3}(\mathbf{r_2} - \mathbf{r_1}) + G\mu_1 M_2 r_2^{-2}\hat{\mathbf{r}}_\mathbf{2}. \tag{2}$$

The first term on the right-hand-side is the direct gravitational acceleration of planet 1 due to planet 2. The second is a frame-acceleration effect, due to the acceleration the Sun feels due to the second planet. Since the Sun is fixed at the zero of the frame, this acceleration is manifested by acceleration in the opposite direction of planet 1. Can we average the force over the 5:2 resonant conjunction timescale, and see what it amounts to for each of the orbital elements?

Likewise, Leverrier and Adams used the same technique, dynamical perturbations, to discover the first planet by gravitational means (Adams 1847; Le Verrier 1877). In this case, they did not know the zeroth order solution (i.e. the Keplerian ellipse) for the yet-to-be-discovered Neptune. In its place, they assumed the Titius-Bode rule held, and sought only the phase of the orbit. This worked because they only wanted to see how the acceleration, then deceleration, as Uranus passed Neptune, would betray its position on the sky to optical observers. [Say later: the task that researchers set for themselves to discover planets by TTV is a bit more demanding. We do not have any hints as to what the planet's orbit might be (neither circular nor roughly obeying some spacing law). Additionally, the data per orbit is considerably noisy; in only a few cases are the orbit-by-orbit "chopping" signal statistically significant after just three transits. Finally, the orbit is only sampled at the transit phase, so opportunities for aliasing of the signal are abundant.]

The discovery of transits marks the first time that data on exoplanets could be precise enough to notice gravitational interactions.[2] The times of transit are primarily constrained by the decline of stellar flux during transit ingress, and the rise over egress, which occur on a timescale

$$\tau \approx \pi^{-1} P(R_p/a) \approx 10^{-4} P \left(\frac{3R_p}{R_\oplus}\right) \left(\frac{a}{0.3\mathrm{AU}}\right)^{-1}, \tag{3}$$

assuming an impact parameter of $b = 0$. This allows the transit times to be measured precisely relative to the orbital period, giving a sensitive measure of the variation of the angular position of a planet relative to a Keplerian orbit. In contrast, the stellar radial velocity varies on the orbital timescale, and thus the precision of the orbital

[2] Only around the same time (2000) were perturbations noticed in the resonant interaction of the planets of GJ 876.

phase is poorly constrained in the absence of high precision or long duration (which allows deviations to grow with time).

- Definition of TTVs/TDVs [DF] (Figure? O-C method) (Holman and Murray 2005; Holman et al 2010)

The literature on exoplanets has a history of rediscovering effects that had been well studied in the field of binary stars. Radial velocity, transits/eclipses, the Rossiter-McLaughlin effect, astrometry, and high-contrast imaging have all been used in the study of multi-star sytems. Stars, however, are only stable in a hierarchical configuration so that only secular or tidal dynamics can play a role in triple star systems (Borkovits et al 2003). Planetary systems can be much more compact due to the dominant mass of the central star, and so mean-motion resonances can dominate the dynamics of multi-planet systems. Transit-timing variations due to mean-motion resonances is a novel aspect of exoplanet systems that did not play a role in the study of multi-star systems.

The first recognition of the importance of transit timing and duration variations was at the DPS and AAS meetings two decades ago by Dobrovolskis and Borucki (1996a,b), followed a few years later by Miralda-Escudé (2002) and Schneider (2003, 2004). More detailed studies which included the important effect of mean-motion resonance were submitted simultaneously by Holman and Murray (2005) and Agol et al (2005). The former paper showed that Solar-system like perturbations might be used to find Earth-like planets, should transit times be measured with sufficient accuracy. The latter paper coined the term 'transit-timing variations,' with acronym TTVs, and defined TTVs as being the residuals of a linear fit to the times of a transiting planet.

Initial studies of TTVs of hot Jupiters were able to place limits on the presence of Earth-mass planets near mean-motion resonance. Some further studies claimed detection of perturbing planets causing TTVs or TDVs, but each of these were quickly disputed or refuted by additional measurements. The first convincing detection awaited the launch of the Kepler spacecraft, and the detection of Kepler-9 which showed large-amplitude TTVs of two Saturn-sized planets with strong significance (Holman et al 2010); this discovery was remarkably similar to predictions that had been made based upon the GJ 876 system (Agol et al 2005). This paper kicked off a series of discoveries of TTVs with the Kepler spacecraft, with now more than 100 systems displaying TTVs, and a handful showing TDVs.

Preliminaries

Since the gravitational interactions between planets occurs on the orbital timescale, the amplitude of transit timing variations is proportional to the orbital period of each planet, as well as a function of other dimensionless quantities. Thanks to Newton's second law and Newton's law of gravity, the acceleration of a body does not depend on its own mass. Thus, the transit timing variations of each planet scale with the

masses of the *other* bodies in the system. In a two-planet system, then, to lowest order in mass ratio,

$$|\delta t_1| = \frac{P_1}{2\pi}\frac{m_2}{m_0} f_{12}(\alpha_{12}, \mathbf{x}_{12}),$$
$$|\delta t_2| = \frac{P_2}{2\pi}\frac{m_1}{m_0} f_{21}(\alpha_{12}, \mathbf{x}_{21}), \quad (4)$$

where the masses of the star and planets are m_0, m_1, and m_2, and f_{ij} governs the timing variations of planet j on planet i, which is a function of the semi-major axis ratio, $\alpha_{12} = a_1/a_2 < 1$, and the angular orbital elements of the planets, $\mathbf{x}_{ij} = (\lambda_i, \omega_i, I_i, \Omega_i, \lambda_j, \omega_j, I_j, \Omega_j)$.

- Energy/angular momentum conservation [DF]

With the addition of multiple perturbing planets, if the mass-ratios of the planets to the star is sufficiently small and if none of the planets exist in a resonant configuration, then the transiting timing variations may be approximately expressed as linear combinations of the perturbations due to each companion. For N planets, the TTVs become

$$\delta t_j = P_j \sum_{i \neq j} \frac{m_i}{m_0} f_{ij}(\alpha_{ij}, \mathbf{x}_{ij}). \quad (5)$$

Note that $\alpha_{ij} = \min(a_i/a_j, a_j/a_i)$.

The measurement of TTVs and TDVs has been used for confirmation, detection, and characterization of transiting exoplanets and their companions. The Kepler spacecraft discovered thousands of transiting exoplanet candidates; the classification as 'candidate' was cautiously used to allow for other possible explanations, such as a blend of a foreground star and a background eclipsing binary causing an apparent transit-like signal. The presence of multiple transiting planets around the same star gave a means of confirming two planets that display *anti-correlated* TTVs: due to energy and angular momentum conservation, the anti-correlation indicates dynamical interactions between the two planets, while such a configuration would not be stable for a triple star system. A series of papers used this technique to confirm that Kepler planet candidates were bonafide exoplanets: Ford et al (2011, 2012a); Fabrycky et al (2012); Ford et al (2012b); Steffen et al (2012, 2013); Xie (2013, 2014).

The confident detection of perturbing exoplanets with TTVs awaited the Kepler spacecraft as well. The Kepler-19b planet showed sinusoidal TTVs that were used to identify a handful of possible planet period and mass combinations that might be responsible for the perturbations (Ballard et al 2011). The unique identification of a perturbing planet was accomplished with Kepler-46 (aka KOI-872) which displayed very high signal-to-noise TTVs which allowed the period and mass of the perturber to be measured with some precision (Nesvorný et al 2012).

The characterization of exoplanets with TTVs also began in earnest with the Kepler spacecraft. In addition to Kepler-9, the Kepler-18 system was characterized by a combination of TTVs and RVs, giving density estimates for the three transiting planets (Cochran et al 2011).

The characterization of exoplanets is complicated by degeneracy between mass and eccentricity caused by aliasing at the frequency of the transiting planet (discussed below). However, in general transit timing variations gives a means of measuring the density of exoplanets. The two observables associated with a light curve are the time stamp of each photometric measurement and the number of photons measured. The number of photons is a dimensionless number, and thus may only constrain dimensionless quantities, such as radius ratio, impact parameter, or the ratio of the stellar size to the semi-major axis. The quantities that have units of time — the period, transit duration, ingress duration — can further constrain the density of the system since the dynamical time $t_{dyn} \approx (G\rho)^{-1/2}$. Seager and Mallén-Ornelas (2003) showed that a single transiting planet on a well-measured circular orbit may be used to gauge the density of the star; in the case of multiple transiting planets, the circular assumption may be relaxed (Kipping 2014). The transit depth, then, gives the radius-ratio of the planet to the star, while if two transit and show TTVs, their TTVs give an estimate of the mass ratio of their perturber to the star. Thus, two transiting, interacting planets yield an estimate of the density ratio of the planets to the star, and consequently we can obtain the density of the planets. Note that this is true even if the absolute mass and radius of the star are poorly constrained. A caveat to this technique is that there is an eccentricity dependence that is present in TTVs as well, but typically multi-transiting planet systems require low eccentricities to be stable, and in some cases the eccentricities can be constrained sufficiently from TTVs, from analyzing multiple planets (Kipping 2014), or statistically from an ensemble analysis (Hadden and Lithwick 2014), so this ends up not impacting the stellar density estimate significantly, although it can impact the planet-star mass ratios, and hence inflate the planet density uncertainty. Another way to obtain an estimate of stellar density is from asteroseismology: in fact, the time dependence of asteroseismic measurements is what enables density to be constrained in that case as well (Ulrich 1986).

If a pair of transiting exoplanets can be detected with *both* TTVs and RVs, then the absolute dimensions of the system can be obtained (Agol et al 2005; Montet and Johnson 2013) as RVs have a dimensions of velocity, which when combined with time measurements from TTVs gives dimensions of distance. In practice this technique has yet to yield useful constraints upon the properties of planetary systems (Almenara et al 2015), but it may prove fruitful in the future much as double-lined spectroscopic binaries have used to measuring the properties of binary stars. Circumbinary planets are an extreme example of this technique: the timing offsets of the transits, combined with the eclipses and radial-velocity of the binary give very precise constraints on the absolute parameters of the Kepler-16 system (Doyle et al 2011).

Theory

- TTVs: - Inner Keplerian variation; CBPs as example (Kepler-16) [DF] - Near-resonant TTVs - Lithwick et al. [DF] (Figure - mechanism + data) - Degeneracy - multiple resonances can give same solution (Kepler-19); Breaking degeneracy with TDV as well [DF]

Chopping

When two planets are nearly resonant, the degeneracy between the mass ratios of the planets to the star and the eccentricity vector may be broken by examining additional non-resonant harmonics present in the data (Deck and Agol 2015). These additional harmonics have a smaller amplitude due to the fact that they are not caused by resonant terms, and thus require higher signal-to-noise to break the degeneracy between the mass and eccentricity. Nevertheless, the chopping component can be detected in many cases, and leads to a unique measurement of the masses of the exoplanets (Schmitt et al 2014; Deck and Agol 2015).

As an example, consider a pair of planets with period ratio of $P_2/P_1 = 1.52$. This period ratio is close to 3:2, and thus is affected by this resonant term, giving a TTV period of $75P_1$. Figure 1 compares two planets with this period ratio with zero eccentricity and mass-ratios of 10^{-6} to a pair of planets with eccentricites of $e_1 = e_2 = 0.04$ and mass-ratios near 10^{-7}. Both pairs of planets give nearly identical amplitudes for the resonant term, while the larger mass ratio planets show a much stronger chopping variation. In this case there is a clear difference between the TTVs of the two simulated systems: the inner planet shows a drift over three orbital periods, and a sudden jump every third orbital period, while the outer one shows a similar pattern over two orbital periods. These variations are due to perturbations at integer multiples of the synodic frequency, which has a period $P_{syn}^{-1} = 1/P_1 - 1/P_2$. In this example we have set the phase of the orbital parameters to be such that the TTVs match; change in the phase can also be indicative of a non-zero eccentricity contributing to the TTVs, and with an ensemble of planets which are believed to have a similar eccentricity distribution, the mass-eccentricity degeneracy may be broken statistically (Lithwick et al 2012; Hadden and Lithwick 2014).

- Resonance - Kepler-30? Ne'svorny (1603.07306); Boue'+2012 - Kepler-223 (resonant chain - to fit data & stability); room for more work on this. [DF] - Exomoons [EA] - Light time? Borkovits deconvolution [DF] - Borkovits(?) - KOI 1474 cleaner example? Or leave out? Future – circumstellar planets in binaries; Schwartz et al. w/ Haghighipour. [DF] - TDVs - Precession - Kepler-108 1606.04485 / KOI-142 Nesvorny / KOI-13 (Mazeh) - and CBPs turning on or off. [DF] Ragozzine/Wolf/Pal/Koscis/Jordan - GR precession - Heyl & Gladman; J2 (Figure - CBP? - Kepler-47? Kostov? Kepler-35? Try them out.)

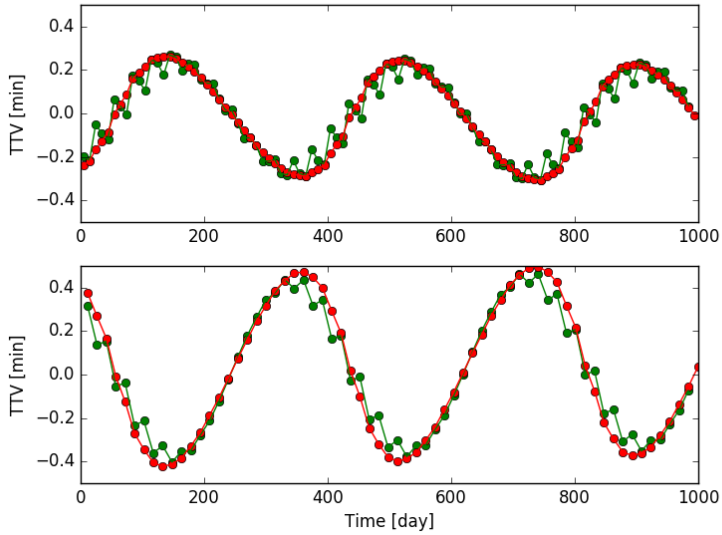

Fig. 1 Transit-timing variations of two low-eccentricity planets with larger mass ratios, $m_1 = m_2 = 10^{-6} m_*$ (green) compared with two higher eccentricity planets ($e_1 = e_2 = 0.04$) with smaller mass ratios $m_1 = m_2 = 10^{-7} m_*$. The zig-zag chopping component is apparent in the high-mass/low-eccentricity case, while less apparent in the low-mass/ high-eccentricity case.

Observations/Practical considerations

Confirmation of multi-planet systems in Kepler anti-correlated sinusoids, Ford GPs [DF]

Timing precision

The steepest portions of a transit are the ingress and egress when the planet crosses onto and off of the disk of the star, causing a dip of depth $\delta = (R_p/R_*)^2$ if we ignore limb-darkening. Suppose for the moment that the only source of noise is Poisson noise due to the count rate of the star, $\dot{N}$. The photometric precision over the duration of ingress scales as $(\dot{N}\tau)^{1/2}$, where τ is the ingress duration (eqn. 3). If the time of ingress fit from a model is offset by σ_g, then the difference in counts observed versus the model is $\sigma_g \delta \dot{N}$ (the pink region in Fig. 2). Equating this to photometric uncertainty gives $\sigma_g = \tau^{1/2} \dot{N}^{-1/2} \delta^{-1}$, which is the 68.3% confidence timing precision assuming that the exposure time is much shorter than the ingress duration and that $\sigma_g \ll \tau$. The same formula applies to egress. A longer transit ingress duration leads to a shallower slope in ingress, which makes it more difficult

to measure an offset in time of the model. Higher count rates and deeper transits improve the precision, as expected. Note that we've assumed that the duration of the transit is sufficiently long that the error on δ is small.

Suppose the transit duration is T. Then, the uncertainty on the duration is given by the sum of the uncertainties on the ingress and egress, added in quadrature: $\sigma_T = \sqrt{2}\sigma_g$. The timing precision, σ_t, is set by the mean of the ingress and egress, giving $\sigma_t = \frac{1}{\sqrt{2}}\sigma_g$.

A more complete derivation of these expressions is given by Carter et al (2008), while an expression which includes the effects of a finite integration time is given by Price and Rogers (2014). The assumptions of no limb-darkening and Poisson noise are generally broken by stars; in addition, stellar variability contributes to timing uncertainty, for which there is yet to be a general expression. These effects generally increase the uncertainty on the measurement of transit times and durations, and so the best practice would be to estimate the timing uncertainties from the data, accounting for effects of correlated stellar variability by including the full covariance matrix of the timing uncertainty (Carter and Winn 2009; Gibson et al 2012). Crossing of the path of the planet across star spots may also cause some uncertainty on the timing precision; this can be diagnosed by a larger scatter within transit than outside transit or other signs of significant stellar activity, and can be handled best by including the spots in the transit model Ioannidis et al (2016).

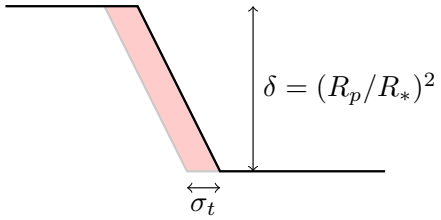

Fig. 2 Diagram of the transit ingress of a planet. The precision of the timing of ingress, σ_g, is set by when the area of the ingress (pink) equals the timing precision over the duration of ingress.

Science Results

- Best characterization, specifically mass: Kepler-36 - conjunctions/impulse/Hill approximation (N-body) [EA]
- Other favorite systems? Kepler-11 puffy/packed planets [DF]
- Best eccentricity constraint for a super-Earth? Kepler-36? Include?
- Ensemble TTV analysis: Xie - differing architecture for the single-transiters due to less frequent TTV, Hadden-Lithwick - eccentricity distribution; Hot Jupiters lonely (Steffen); Latham - gas giants less frequent in multi-transiting (no TTVs) [DF]
- Measuring masses - Steffen bias? [DF]

- N-body modeling of Kepler-systems: Jontof-Hutter [DF] (Mass-radius Figure? - ask Daniel Jontof-Hutter) Transparency to avoid big error bars visually dominating. EA will make the figure. Referenced Wayne Hu figure on cosmo constraints.
- CBPs [DF]

Future

- More thorough TTV analysis: GPs - for measuring transit times - Follow-up of Kepler targets - Comparison of TTV masses with RV masses: better constraints and confidence in both methods? - MCMC with high-multiplicity systems - TESS, JWST, CHEOPS, PLATO, ? - TTV/TDV of exomoons - HZ exoplanets - Smaller CBPs - Stellar/planet characterization: TTV + RV

References:

Borucki & Summers Struve Cabrera Charbonneau 2000

Neptune: Bouvard/Adams/Le Verrier/Galle

Acknowledgements EA acknowledges support from NASA Grant ... DCF acknowledges support from...

References

Adams JC (1847) An Explanation of the Observed Irregularities in the Motion of Uranus, on the Hypothesis of Disturbances caused by a more Distant Planet; with a Determination of the Mass, Orbit, and Position of the Disturbing Body. MmRAS16:427

Agol E, Steffen J, Sari R Clarkson W (2005) On detecting terrestrial planets with timing of giant planet transits. MNRAS359:567–579, DOI 10.1111/j.1365-2966.2005.08922.x, astro-ph/0412032

Almenara JM, Díaz RF, Mardling R et al (2015) Absolute masses and radii determination in multiplanetary systems without stellar models. MNRAS453:2644–2652, DOI 10.1093/mnras/stv1735, 1508.06596

Ballard S, Fabrycky D, Fressin F et al (2011) The Kepler-19 System: A Transiting 2.2 R$_\oplus$ Planet and a Second Planet Detected via Transit Timing Variations. ApJ743:200, DOI 10.1088/0004-637X/743/2/200, 1109.1561

Borkovits T, Érdi B, Forgács-Dajka E Kovács T (2003) On the detectability of long period perturbations in close hierarchical triple stellar systems. A&A398:1091–1102, DOI 10.1051/0004-6361:20021688

Carter JA Winn JN (2009) Parameter Estimation from Time-series Data with Correlated Errors: A Wavelet-based Method and its Application to Transit Light Curves. ApJ704:51–67, DOI 10.1088/0004-637X/704/1/51, 0909.0747

Carter JA, Yee JC, Eastman J, Gaudi BS Winn JN (2008) Analytic Approximations for Transit Light-Curve Observables, Uncertainties, and Covariances. ApJ689:499-512, DOI 10.1086/592321, 0805.0238

Cochran WD, Fabrycky DC, Torres G et al (2011) Kepler-18b, c, and d: A System of Three Planets Confirmed by Transit Timing Variations, Light Curve Validation, Warm-Spitzer Pho-

tometry, and Radial Velocity Measurements. ApJS197:7, DOI 10.1088/0067-0049/197/1/7, 1110.0820

Deck KM Agol E (2015) Measurement of Planet Masses with Transit Timing Variations Due to Synodic "Chopping" Effects. ApJ802:116, DOI 10.1088/0004-637X/802/2/116, 1411.0004

Dobrovolskis AR Borucki WJ (1996a) Influence of Jovian Extrasolar Planets on Transits of Inner Planets. In: AAS/Division for Planetary Sciences Meeting Abstracts #28, Bulletin of the American Astronomical Society, vol 28, p 1112

Dobrovolskis AR Borucki WJ (1996b) Influence of Jovian extrasolar planets on transits of inner planets. In: Bulletin of the American Astronomical Society, BAAS, vol 28, p 1112

Doyle LR, Carter JA, Fabrycky DC et al (2011) Kepler-16: A Transiting Circumbinary Planet. Science 333:1602, DOI 10.1126/science.1210923, 1109.3432

Fabrycky DC, Ford EB, Steffen JH et al (2012) Transit Timing Observations from Kepler. IV. Confirmation of Four Multiple-planet Systems by Simple Physical Models. ApJ750:114, DOI 10.1088/0004-637X/750/2/114, 1201.5415

Ford EB, Rowe JF, Fabrycky DC et al (2011) Transit Timing Observations from Kepler. I. Statistical Analysis of the First Four Months. ApJS197:2, DOI 10.1088/0067-0049/197/1/2, 1102.0544

Ford EB, Fabrycky DC, Steffen JH et al (2012a) Transit Timing Observations from Kepler. II. Confirmation of Two Multiplanet Systems via a Non-parametric Correlation Analysis. ApJ750:113, DOI 10.1088/0004-637X/750/2/113, 1201.5409

Ford EB, Ragozzine D, Rowe JF et al (2012b) Transit Timing Observations from Kepler. V. Transit Timing Variation Candidates in the First Sixteen Months from Polynomial Models. ApJ756:185, DOI 10.1088/0004-637X/756/2/185, 1201.1892

Gibson NP, Aigrain S, Roberts S et al (2012) A Gaussian process framework for modelling instrumental systematics: application to transmission spectroscopy. MNRAS419:2683–2694, DOI 10.1111/j.1365-2966.2011.19915.x, 1109.3251

Hadden S Lithwick Y (2014) Densities and Eccentricities of 139 Kepler Planets from Transit Time Variations. ApJ787:80, DOI 10.1088/0004-637X/787/1/80, 1310.7942

Holman MJ Murray NW (2005) The Use of Transit Timing to Detect Terrestrial-Mass Extrasolar Planets. Science 307:1288–1291, DOI 10.1126/science.1107822, astro-ph/0412028

Holman MJ, Fabrycky DC, Ragozzine D et al (2010) Kepler-9: A System of Multiple Planets Transiting a Sun-Like Star, Confirmed by Timing Variations. Science 330:51, DOI 10.1126/science.1195778

Ioannidis P, Huber KF Schmitt JHMM (2016) How do starspots influence the transit timing variations of exoplanets? Simulations of individual and consecutive transits. A&A585:A72, DOI 10.1051/0004-6361/201527184, 1510.03276

Kipping DM (2014) Characterizing distant worlds with asterodensity profiling. MNRAS440:2164–2184, DOI 10.1093/mnras/stu318, 1311.1170

Le Verrier UJ (1877) Tables du mouvement de Neptune fondees sur la comparaison de la theorie avec les observations. Annales de l'Observatoire de Paris 14:1

Lithwick Y, Xie J Wu Y (2012) Extracting Planet Mass and Eccentricity from TTV Data. ApJ761:122, DOI 10.1088/0004-637X/761/2/122, 1207.4192

Miralda-Escudé J (2002) Orbital Perturbations of Transiting Planets: A Possible Method to Measure Stellar Quadrupoles and to Detect Earth-Mass Planets. ApJ564:1019–1023, DOI 10.1086/324279, astro-ph/0104034

Montet BT Johnson JA (2013) Model-independent Stellar and Planetary Masses from Multi-transiting Exoplanetary Systems. ApJ762:112, DOI 10.1088/0004-637X/762/2/112, 1211.4028

Nesvorný D, Kipping DM, Buchhave LA et al (2012) The Detection and Characterization of a Nontransiting Planet by Transit Timing Variations. Science 336:1133, DOI 10.1126/science.1221141, 1208.0942

Price EM Rogers LA (2014) Transit Light Curves with Finite Integration Time: Fisher Information Analysis. ApJ794:92, DOI 10.1088/0004-637X/794/1/92, 1408.4124

Schmitt JR, Agol E, Deck KM et al (2014) Planet Hunters. VII. Discovery of a New Low-mass, Low-density Planet (PH3 C) Orbiting Kepler-289 with Mass Measurements of Two Additional Planets (PH3 B and D). ApJ795:167, DOI 10.1088/0004-637X/795/2/167, 1410.8114

Schneider J (2003) Multi-planet system detection by transits. In: Combes F, Barret D, Contini T Pagani L (eds) SF2A-2003: Semaine de l'Astrophysique Francaise, p 149

Schneider J (2004) Multi-planet system detection with Eddington. In: Favata F, Aigrain S Wilson A (eds) Stellar Structure and Habitable Planet Finding, ESA Special Publication, vol 538, pp 407–410

Seager S Mallén-Ornelas G (2003) A Unique Solution of Planet and Star Parameters from an Extrasolar Planet Transit Light Curve. ApJ585:1038–1055, DOI 10.1086/346105, astro-ph/0206228

Steffen JH, Fabrycky DC, Ford EB et al (2012) Transit timing observations from Kepler - III. Confirmation of four multiple planet systems by a Fourier-domain study of anticorrelated transit timing variations. MNRAS421:2342–2354, DOI 10.1111/j.1365-2966.2012.20467.x, 1201.5412

Steffen JH, Fabrycky DC, Agol E et al (2013) Transit timing observations from Kepler - VII. Confirmation of 27 planets in 13 multiplanet systems via transit timing variations and orbital stability. MNRAS428:1077–1087, DOI 10.1093/mnras/sts090, 1208.3499

Ulrich RK (1986) Determination of stellar ages from asteroseismology. ApJ306:L37–L40, DOI 10.1086/184700

Xie JW (2013) Transit Timing Variation of Near-resonance Planetary Pairs: Confirmation of 12 Multiple-planet Systems. ApJS208:22, DOI 10.1088/0067-0049/208/2/22, 1208.3312

Xie JW (2014) Transit Timing Variation of Near-resonance Planetary Pairs. II. Confirmation of 30 Planets in 15 Multiple-planet Systems. ApJS210:25, DOI 10.1088/0067-0049/210/2/25, 1309.2329